Partial Oxidation of Methane Over Co-ZSM-5: Tuning the Oxygenate Selectivity by Altering the Preparation Route

Nadzeya V. Beznis · Bert M. Weckhuysen ·
Johannes H. Bitter

Abstract For the first time the possibility to partially oxidize methane to methanol and formaldehyde at low temperature over Co-ZSM-5 using air is shown. The influence of the preparation method on the nature of the cobalt species is investigated. In addition, the catalytic activity and selectivity for methane oxidation as a function of the cobalt speciation is discussed. Based on UV–vis–NIR and FT-IR spectroscopy, H_2-TPR, TEM and kinetic measurements it is concluded that cobalt in ion-exchange positions results mainly in the formation of formaldehyde, while larger Co-oxide particles prepared by impregnation result in the formation of methanol.

1 Introduction

The direct conversion of methane to methanol and formaldehyde holds one of the greatest challenges in heterogeneous catalysis [1–4]. Methane is an important fossil feedstock and its direct partial oxidation to oxygenates is challenging for thermodynamic reasons. Currently, oxygenates (e.g. methanol) are prepared from methane via a multi-step process. First syn-gas (CO and H_2) is generated followed by the oxygenate formation in a second step [5–7]. Though these processes are highly efficient, methanol synthesis following this route is only economically viable when performed on a large scale, which is the result of high capital costs for syn-gas production [8]. Obviously,

a more convenient way for small-scale methanol production would be the direct synthesis of methanol from methane making use of air or oxygen.

Fe-ZSM-5 is known to be active for this conversion although N_2O was indispensable as oxidant [9, 10]. Due to the limited availability of N_2O the use of molecular oxygen or air as an oxidant is more attractive. Recently, it was reported that Cu-ZSM-5 was able to perform the methane to methanol reaction. However, a preliminary calcination to introduce active oxygen is required. It is also necessary to mention here that the methanol formation is not continuous yet and an extraction procedure is needed [11, 12]. An initial screening study in our laboratory showed that especially Co-ZSM-5 displays intriguing catalytic behavior in the partial oxidation of methane to oxygenates. We will show in this work that Co-ZSM-5, preliminary calcined in air, can convert methane to methanol and/or formaldehyde.

Co-ZSM-5 can be prepared by different methods: wet ion-exchange [13–15], solid-state ion-exchange [16, 17], incipient wetness impregnation [14, 17] and sublimation [17]. The preparation method determines the cobalt species present in materials. Cobalt-loaded ZSM-5 samples may contain at least two cobalt species: Co^{2+} in ion-exchange position and cobalt oxidic species. These cobalt species exhibit different catalytic [18–20] and magnetic [14] properties.

We chose to prepare Co-ZSM-5 materials by wet ion-exchange and incipient wetness impregnation. UV–vis–NIR Diffuse Reflectance (DR) spectroscopy, Fourier Transform Infrared Spectroscopy (FT-IR), Temperature Programmed Reduction (H_2-TPR) and Transmission Electron Microscopy (TEM) were used to identify the nature of the Co-species present in these samples. The characterization results were related to the catalytic behavior of the samples in order to establish a qualitative

N. V. Beznis · B. M. Weckhuysen · J. H. Bitter (✉)
Inorganic Chemistry and Catalysis Group, Department of
Chemistry, Debye Institute for Nanomaterials Science, Utrecht
University, Sorbonnelaan 16, 3584 CA Utrecht, The Netherlands
e-mail: j.h.bitter@uu.nl

structure-performance relation for the production of oxygenates over Co-ZSM-5 using methane and air.

2 Experimental Part

NH$_4$-ZSM-5 (ZEOLYST, Si/Al = 17.5) was converted to Na-ZSM-5 via ion-exchange using 0.1 M NaNO$_3$ (98%, Acros Organics) at ambient temperature (RT) for 24 h; the procedure was repeated three times. Ion-exchanged Co-ZSM-5 catalysts were prepared using an aqueous solution of 0.02 M cobalt acetate (98%, Acros Organics) or cobalt nitrate (98%, Acros Organics) for 24 h. This procedure was performed both at RT and at 80 °C. After loading the samples were washed with demineralised water and dried at 120 °C in static air. In addition, Co-ZSM-5 samples were also prepared by incipient wetness impregnation using either a 0.05 M cobalt nitrate or acetate solution. After metal-loading the samples were dried at 60 °C in a flow of N$_2$. The cobalt loading was determined by Atomic Absorption Spectroscopy (AAS).

For activation the samples were calcined at 550 °C for 3 h in flow of N$_2$ (800 mL/min) and O$_2$ (200 mL/min) with a ramp of 0.5 °C/min [21, 22]. After calcination the reaction with methane was performed (at 150 °C for 25 min in 8% CH$_4$ in He with total flow 25 mL/min) in a batch mode. Activation and reaction were performed in a quartz flow cell equipped with a UV–vis–NIR transparent window.

The analysis of the gas leaving the reactor was carried out using an Interscience Compact GC system, equipped with two different columns a Molsieve 5A and a Porabond Q columns each having a TCD detector.

After reaction with methane an extraction procedure was performed by stirring 0.2 g of the sample in 0.5 mL ethanol for 1 h. A Shimadzu GC 2010 with CP-WAX 52 CB column and liquid sampler AOC—20i was used to quantify the product concentrations in the samples.

Both after calcination and after exposing to methane UV–vis–NIR Diffuse Reflectance (DR) spectra of the samples were recorded on a Varian Cary 500 spectrometer in the range 5,000–50,000 cm^{-1} (200–2,200 nm). In order to eliminate the contributions of the zeolite material, a DR UV–vis–NIR spectrum of dehydrated ZSM-5 zeolite sample was subtracted of all Co-ZSM-5 samples.

The nature of surface species on the catalyst after exposing to methane was also investigated using Fourier Transform Infrared Spectroscopy (FT-IR). Samples, pressed into self-supporting wafers, were heated in He with a temperature ramp of 2 °C/min to 200 °C. Infrared spectra were recorded in a He flow at 200 °C on a Perkin Elmer FT-IR 2000 spectrometer using a DTGS detector. Twenty-five scans were averaged and data were baseline corrected and the intensity of each spectrum was normalized at the zeolite overtones (1,850–1,950 cm^{-1}).

X-Ray Diffraction (XRD) patterns of the Co-ZSM-5 materials were recorded on a Nonius PDS 120 powder diffraction apparatus with Co Kα radiation ($\lambda = 1.78897$ Å).

For Transmission Electron Microscopy (TEM) measurements small amount of the sample was positioned on a carbon microgrid supported on copper. The microscope Tecnai 20 (FEI) equipped with a field emission gun was operated at 200 kV. Elemental composition was obtained by Energy Dispersive analysis of X-rays (EDX) performed through a LINK EDX system.

Temperature Programmed Reduction (H$_2$-TPR) was executed on an Autochem 2920 instrument from Micrometrics. 0.8 g catalyst was heated with a rate of 5 °C/min in 5% H$_2$ in Ar (50 mL/min). Before the experiment the samples were dried in Ar at 120 °C for 1 h.

3 Results and Discussion

Co-ZSM-5 (Si/Al–17.5) samples were prepared either by aqueous ion-exchange at RT or 80 °C, using either cobalt acetate or cobalt nitrate, or by incipient wetness impregnation also using an aqueous solution of cobalt nitrate or cobalt acetate (Table 1).

After drying the samples were in situ activated in air by a mild calcination procedure [21, 22] i.e., in a high gas-flow rate (1,000 mL/min) with a low temperature ramp (0.5 °C/min). In that way the highest possible amount of moisture was removed at a relatively low temperature, while preventing metal ion clustering. The XRD patterns of all cobalt loaded ZSM-5 samples after calcination appeared to be identical, indicating no detectable damage of the ZSM-5 structure. No additional peaks due to the presence of cobalt oxide phases were found within the experimental sensitivity of XRD.

The nature of the cobalt species present can be visualized by means of UV–vis–NIR DR spectroscopy after calcinations and after reaction with methane. A UV–vis–NIR DR spectrum of calcined Co-IE_RT_A_0.9 is shown in Fig. 1A. Two triplet bands are visible. The first triplet is

Table 1 Overview of the samples under investigation, the sample loadings and their preparation method

Sample	Preparation	Cobalt precursor	Co (wt%)[a]
Co_IE_RT_A_0.9	Ion-exchange at RT	Cobalt acetate	0.9
Co_IE_RT_N_0.6	Ion-exchange at RT	Cobalt nitrate	0.6
Co_IE_80_A_2.7	Ion-exchange at 80 °C	Cobalt acetate	2.7
Co_IE_80_N_1.7	Ion-exchange at 80 °C	Cobalt nitrate	1.7
Co_IMP_A_2.5	Impregnation	Cobalt acetate	2.5
Co_IMP_N_2.5	Impregnation	Cobalt nitrate	2.5

[a] Determined by atomic absorbance spectroscopy
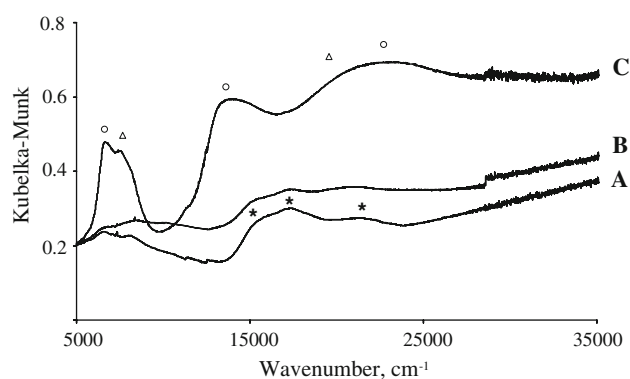
Fig. 1 The UV–vis–NIR DR spectra of Co_IE_RT_A_0.9 (*A*); Co_IE_80_A_2.7 (*B*) and Co_IMP_N_2.5 (*C*) after calcination at 550 °C (*asterisk* isolated Co^{2+}: $^4A_2(F) \rightarrow {}^4T_1(P)$ transition; *circle* Co_3O_4: $^1A_{1g} \rightarrow {}^1T_{2g}$ and $^1A_{1g} \rightarrow {}^1T_{1g}$ transitions; *triangle* CoO: $^1T_{1g}(F) \rightarrow {}^1T_{2g}(F)$ and $^1T_{1g}(F) \rightarrow {}^1T_{1g}(P)$ transitions)

in the near infrared (NIR) region (5,000, 6,500 and 8,000 cm^{-1}). This triplet could be assigned to the $^4A_2(F) \rightarrow {}^4T_1(F)$ transition [23]. However, in the NIR region, the cobalt spectra might be overlapped by the overtone bands of OH groups (7,200–7,400 cm^{-1}) and water molecules (5,200 cm^{-1}). Therefore, the NIR region is usually used to check the dehydration of zeolites, while the vis region is used to monitor the nature of the cobalt species [13]. The second triplet (marked with asterisk) is observed in the visible region (15,000, 17,000 and 21,500 cm^{-1}) and is ascribed to the $^4A_2(F) \rightarrow {}^4T_1(P)$ transition [23]. Wichterlová et al. [13, 24] assigned the bands in the visible range to Co^{2+} located at three different sites in the ZSM-5, i.e., α-, β- and γ-sites, respectively. The UV–vis–NIR DR spectrum of Co_IE-RT_N_0.6 is identical to Co_IE_RT_A_0.9 and is therefore not shown.

A UV–vis–NIR DR spectrum of Co_IMP_N_2.5 is displayed in Fig. 1C. The broad band between 18,000 and 26,000 cm^{-1} and the band around 13,500 cm^{-1} (marked with circles) are indicative for Co_3O_4 clusters and they are ascribed to octahedral Co^{3+} ($^1A_{1g} \rightarrow {}^1T_{2g}$ and $^1A_{1g} \rightarrow {}^1T_{1g}$ transitions) [25–27]. The band at 8,000 cm^{-1} and the band at around 19,600 cm^{-1} (marked with triangles) are ascribed to the $^1T_{1g}(F) \rightarrow {}^1T_{2g}(F)$ and $^1T_{1g}(F) \rightarrow {}^1T_{1g}(P)$ respectively and indicate the presence of CoO [28]. Therefore, it is concluded that samples prepared by aqueous impregnation contain mainly cobalt oxide species, both

CoO and Co_3O_4. Similar observations were made by impregnation, using cobalt acetate as a precursor.

The samples prepared by ion-exchange at 80 °C have higher metal loadings (2.7 and 1.7 wt%, using cobalt acetate and cobalt nitrate, respectively) in comparison with the samples prepared by ion-exchange at RT (0.9 and 0.6 wt%, using cobalt acetate and cobalt nitrate, respectively) (Table 1). Figure 1B shows a UV–vis–NIR DR spectrum of Co_IE_80_A_2.7. Three bands at 15,000, 17,000 and 21,500 cm^{-1} indicate the presence of Co^{2+} in ion-exchange position as discussed above. In addition the broad between 18,000 and 26,000 cm^{-1} indicate the presence of Co_3O_4. Co_IE_80_N_1.7 also showed the formation of both species.

To give a quantification of the different Co-species present in the samples H$_2$-TPR measurements were performed. Based on the literature, three regions of reduction can be expected, i.e., below 400 °C representing the reduction of extraframework bulk-like Co_3O_4 particles; between 400 and 700 °C representing the reduction of intraframework $(CoO_x)_n$ oligomers containing Co^{2+}; and peaks between 700 and 900 °C representing the reduction of extraframework cobalt (II) phyllosilicate (Table 2). Isolated Co^{2+} can only be reduced above 900 °C. Their quantity was, in general, calculated by the difference between the total amount of cobalt and the amount of cobalt quantified based on the thermograms [29–31].

Table 2 presents the quantification of cobalt species using H$_2$-TPR analysis. For the Co_IE_RT_A_0.9 sample isolated Co^{2+} are the main cobalt species (80%), which is in a good agreement with the UV–vis–NIR DR data. For Co_IMP_N_2.5 we observed mainly cobalt oxide species (85%). Co_IE_80_A_2.7 is an intermediate case and showed 25% of Co-oxide species, 50% isolated Co^{2+} and 25% cobalt phyllosilicate.

The H$_2$-TPR results confirmed UV–vis–NIR DR results and also give the quantification of cobalt species present in Co-ZSM-5 materials.

These findings are also supported by TEM, as indicated in Fig. 2. For Co_IE_RT_A_0.9 (Fig. 2a) no cobalt-containing particles on the outer surface of the zeolite could be found. An EDX analysis confirmed the presence of cobalt throughout the sample suggesting that most cobalt was distributed inside the ZSM-5 channels. Please note that prolonged exposure (few minutes) of the samples resulted

Table 2 H$_2$-TPR results of Co-ZSM-5 samples prepared by different methods

Sample	T_{1max} (°C)	T_{2max} (°C)	T_{3max} (°C)	% Co^{x+} in Co_3O_4 (T_1)	% Co^{2+} in CoO (T_2)	% $CoSiO_4$ (T_3)	% Isolated Co^{2+}
Co_IE_RT_A_0.9	360	690	–	10	10	–	80
Co_IE_80_A_2.7	350	670	805	10	15	25	50
Co_IMP_N_2.5	325	700	–	35	50	–	15

Fig. 2 TEM micrographs of
Co_IE_RT_A_0.9 (**a**),
Co_IE_80_A_2.7 (**b**) and
Co_IMP_N_2.5 (**c**) (cobalt
oxide particles are encircled)
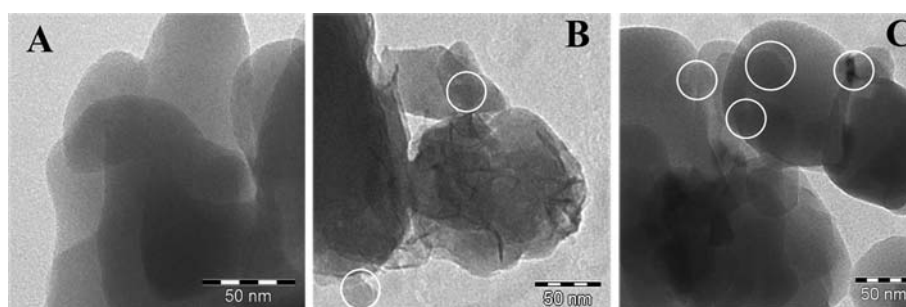
in large cobalt-containing particles (2–5 nm) most likely as the result of Co migration and sintering from the pores to the external surface.

Figure 2b, c show TEM images of Co_IE_80_A_2.7 and Co_IMP_N_2.5, respectively. Large cobalt oxide particles (10–50 nm) were observed for both samples. Areas, where no particles were visible, were also present.

In case of Co_IE_80_A_2.7 cobalt species in needle like structures were observed. This gives an additional confirmation of the presence of cobalt silicate in that sample [30, 32].

To check the catalytic activity after calcination the activated samples were exposed to methane (8% CH_4 in He at 150 °C for 25 min). The gas phase was analyzed during the experiments and indicated that no gaseous products were formed. It is necessary to mention that UV–vis–NIR DR spectra of all prepared Co-ZSM-5 materials after exposure to methane did not show significant difference as compared to the activated sample.

Since the products of the reaction strongly adsorb on the surface of the catalyst an extraction procedure is needed to evaluate the catalytic activity of the samples. The extraction was performed with ethanol. GC analyses were performed to check the amount of formed products.

Figure 3 summarize the catalytic activity and selectivity of the different Co-ZSM-5 samples under investigation. The Co_IE_RT_N_0.6 sample was not active for methane oxidation for unknown reasons. However, Co_IE_RT_A_0.9 with 80% isolated Co^{2+} shows the formation of two products: methanol and formaldehyde, with 75% selectivity towards formaldehyde. Samples prepared by impregnation, using either cobalt acetate or cobalt nitrate as metal precursor, i.e., possessing 85% of the cobalt as oxidic species, were 100% selective towards methanol.

Cobalt samples prepared by ion-exchange at 80 °C (Co_IE_80_A_2.7 and Co_IE_80_N_1.7), having both oxidic Co-species and isolated Co^{2+} species, show the formation of both products: methanol and formaldehyde. Co_IE_80_N_1.7 was 40% selective towards methanol and 60% selective towards formaldehyde, which is similar to that of Co_IE_80_A_2.7 (45% methanol and 55% formaldehyde).
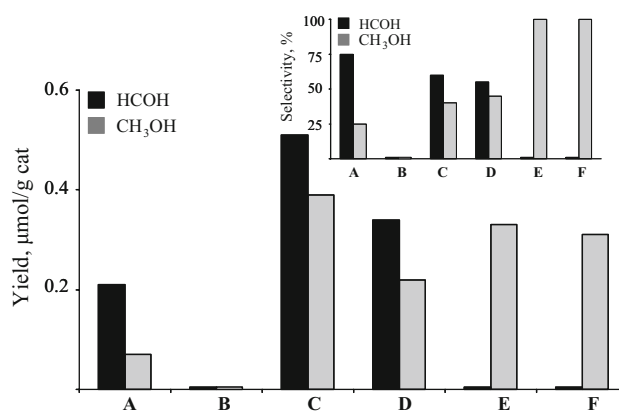

Fig. 3 Catalytic activity and selectivity (insert) of Co-ZSM-5 samples for methane oxidation to oxygenates: Co_IE_RT_A_0.9 (*A*); Co_IE_RT_N_0.6 (*B*); Co_IE_80_A_2.7 (*C*); Co_IE_80_N_1.7 (*D*); Co_IMP_N_2.5 (*E*) and Co_IMP_A_2.5 (*F*)

In addition, it should be mentioned here that it is possible to regenerate the catalyst. After extraction in ethanol the Co-ZSM-5 materials were dried and calcined in air as described above and reused in a second cycle. Similar activities were observed as in previous run.

As it was discussed above, the products of the reaction strongly adsorb on the surface of the catalyst. Thus, we speculate that the strongly adsorbed species are methoxy species. It is known that the formation of a methoxy species (–OCH_3) is generally considered as one of the first steps in chemisorption of methane on an oxidic surface [33, 34]. The formation of methoxy species was indeed confirmed by FT-IR measurements (Fig. 4). Vibrations at around 2,950 and 2,980 cm^{-1} are related to asymmetric CH stretching modes. Symmetric CH stretching vibration were found around 2,850 cm^{-1} [42, 43], and the band at 2,980 cm^{-1} is related to a center rotational band. The positions of the bands were similar for all Co-ZSM-5 samples.

Thus, by relating the catalytic results with UV–vis, H_2-TPR and TEM data we can summarize that the sample which only contained monoatomic Co^{2+} in ion-exchanged positions (Co_IE_RT_A_0.9) is the most selective towards formaldehyde formation. By increasing the amount of
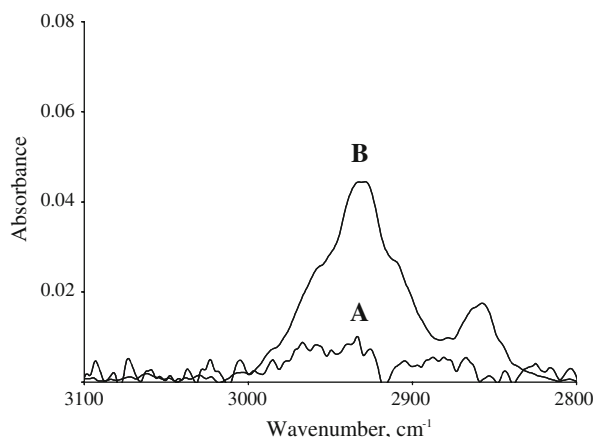
Fig. 4 FT-IR spectra of Co_IE_80_A_2.7 in a He flow at 200 °C before reaction with methane (*A*) and after exposure to methane (*B*)

oxidic cobalt species i.e., samples prepared either by ion-exchange at 80 °C or by impregnation, the selectivity towards methanol increased thus indicating that the presence of oxidic cobalt species relate to the semi qualitative methanol production.

4 Conclusions

Co-ZSM-5 samples are able to partially oxidize methane to oxygenates in one step at low temperature using air as an oxidant. Using different preparation methods it is possible to tune the catalytic activity and selectivity of the catalytic system. In the samples prepared by ion-exchange at RT most cobalt was found to be in ion-exchange positions. These samples were most selective towards formaldehyde. Instead, impregnated samples, containing mainly oxidic cobalt species (CoO and Co_3O_4), are more selective towards methanol.

References

1. Periana RA, Taube DJ, Evitt ER, Löffler DG, Wentreck PR, Voss G, Masuda T (1993) Science 259:340
2. Liu H-F, Liu R-S, Liew KY, Johnson RE, Lunsford JH (1984) J Am Chem Soc 106:4117
3. Li F, Yuan G (2005) Chem Commun 17:2238
4. Bar-Nahum I, Khenkin AM, Neumann R (2004) J Am Chem Soc 126:10236
5. Osako T, Watson EJ, Dehestani A, Bales BC, Mayer JM (2006) Angew Chem Int Ed 45:7433
6. Bañares MA, Cardoso JH, Hutchings GJ, Correa Bueno JM, Fierro JLG (1998) Catal Lett 56:149
7. Liu Z-P, Hu P (2002) J Am Chem Soc 124:11568
8. Poels EK, Brands DS (2000) Appl Catal A Gen 191:83
9. Sobolev VI, Dubkov KA, Panna OV, Panov GI (1995) Catal Today 24:251
10. Panov GI, Kharitonov AS, Sobolev VI (1993) Appl Catal 98:1
11. Groothaert MH, Smeets PJ, Sels BF, Jacobs PA, Schoonheydt RA (2005) J Am Chem Soc 127:1394
12. Smeets PJ, Groothaert MH, Schoonheydt RA (2005) Catal Today 110:303
13. Dědeček J, Kaucký D, Wichterlová B (2000) Micropor Mesopor Mater 35–36:483
14. Pierella LB, Saux C, Caglieri SC, Bertorello HR, Bercoff PG (2008) Appl Catal A Gen 347:55
15. Montanari T, Bevilacqua M, Resini C, Busca G, Pirone R, Ruoppolo G (2007) J Porous Mater 14:291
16. da Cruz RS, Macarenhas AJS, Andrade HMC (1998) Appl Catal B Environ 18:223
17. Wang X, Chen H, Sachtler WMH (2000) Appl Catal B Environ 26:L227
18. Lee C, Chong P, Lee Y, Chin C, Kevan L (1997) Micropor Mater 12:21
19. Moreno-Tost R, Santamaría-Gonzales J, Maireles-Torres P, Rodriquez-Castellón E, Jimenez-López A (2002) Appl Catal B Environ 38:51
20. Bulánek R, Novoveská K, Wichterlová B (2002) Appl Catal A Gen 235:181
21. Battiston AA, Bitter JH, de Groot FMF, Overweg AR, Stephan O, van Bokhoven JA, Kooyman PJ, van der Spek C, Vanko G, Koningsberger DC (2003) J Catal 213:251
22. de Graaf J, van Dillen AJ, de Jong KP, Koningsberger DC (2001) J Catal 203:307
23. Verberckmoes AA, Weckhuysen BM, Schoonheydt RA (1998) Micropor Mesopor Mater 22:165
24. Kaucký D, Dědeček J, Wichterlová B (1999) Micropor Mesopor Mater 31:75
25. Vakros J, Kordulis C, Lycourghiotis A (2002) Langmuir 18:417
26. Liotta LF, Pantaleo G, Macaluso A, Di Carlo G, Deganello G (2003) Appl Catal A Gen 245:167
27. van de Water LGA, Bezemer GL, Bergwerff JA, Versluijs-Helder M, Weckhuysen BM, de Jong KP (2006) J Catal 242:287
28. lever ABP (1984) Inorganic electronic spectroscopy, 2nd edn. Elsevier, Amsterdam
29. Boubaker HB, Mhamdi M, Marceau E, Khaddar-Zine S, Ghorbel A, Che M, Taarit YB, Villain F (2006) Micropor Mesopor Mater 92:62
30. Mhamdi M, Marceau E, Khaddar-Zine S, Ghorbel A, Che M, Taarit YB, Villain F (2004) Catal Lett 98:135
31. de Cruz RS, Mascarenhas AJS, Andrade HMC (1998) Appl Catal B 18:223
32. Chupin C, van Veen AC, Konduru M, Després J, Mirodatos C (2006) J Catal 241:103
33. Finocchio E, Busca G, Lorenzelli V, Willey RJ (2001) J Catal 151:204
34. Steghuis AG, van Ommen JG, Seshan K, Lercher JA (1997) Stud Surf Sci Catal 107:403